SCIENCE CHINA
Technological Sciences

August 2012 Vol.55 No.8: 2184–2190
doi: 10.1007/s11431-012-4892-8

Vertically oriented TiO_2 nanotube arrays with different anodization times for enhanced boiling heat transfer

XU Jia[1*], YANG MingJie[2], XU JinLiang[1*] & JI XianBing[1]

[1] *Beijing Key Laboratory of Low-Grade Energy Multiphase Flow and Heat Transfer, School of Renewable Energy, North China Electric Power University, Beijing 102206, China;*
[2] *Laboratory of Advanced Materials, Department of Material Science and Engineering, Tsinghua University, Beijing 100084, China*

Received October 31, 2011; accepted April 24, 2012; published online May 12, 2012

Pool boiling of saturated water on a plain Ti surface and surfaces covered with vertically-oriented TiO_2 nanotube arrays (NTAs) has been studied. The technique of potentiostatic anodization using non-aqueous electrolytes was adopted to fabricate three types of TiO_2 NTAs distinguished by their anodization time. Compared to the bare Ti surface, the incipient boiling wall superheat on the TiO_2 NTAs was decreased by 11 K. Both the critical heat flux and heat transfer coefficient of pool boiling on the TiO_2 NTAs were higher than those from boiling on a bare Ti surface. The measured maximum critical heat flux and heat transfer coefficient values were 186.7 W/cm^2 and 6.22 W/cm^{2}K, respectively. Different performances for the enhancement of heat transfer by the three types of TiO_2 NTAs were attributed to the different degrees of deformation in the nanostructure during boiling. Long-term performance of the nanomaterial-coated surfaces for enhanced pool boiling showed degradation of the TiO_2 NTAs prepared with an anodization time of 3 hours.

TiO_2 nanotube arrays, pool boiling, heat transfer enhancement, deformation of nanostructure

Citation: Xu J, Yang M J, Xu J L, et al. Vertically oriented TiO_2 nanotube arrays with different anodization times for enhanced boiling heat transfer. Sci China Tech Sci, 2012, 55: 2184–2190, doi: 10.1007/s11431-012-4892-8

1 Introduction

Due to the rapid increase in energy demand worldwide, intensifying heat transfer processes and reducing energy losses have become increasingly important. As a liquid-vapour phase transition mechanism for the efficient conversion of thermal energy, boiling is widely used in a variety of heat-transfer and chemical reaction applications [1–3]. Pool boiling is a classic boiling process, and the intensification of heat transfer in the pool boiling process has been researched extensively over the past few decades [4]. Many techniques have been adopted to modify the shape and roughness of the heated surface to enhance heat transfer, such as mechanical treatment [5], chemical etching [6], electrodepositing [7] and coating with a porous layer of a chosen material [8].

With the development of nanotechnology, fabrication methods, physical properties and industrial applications of nanomaterials have become the focus of interdisciplinary research. Recently, there has been an increasing interest in evaluating the pool boiling performance of nanomaterial-coated surfaces. Arrays consisting of carbon nanotubes [9], Cu and Si nanowires [10] and Cu nanorods [11] have confirmed that boiling performance can be promoted by nano-coated surfaces. Nano-coated surfaces are believed to have more cavities for bubbles to nucleate, larger effective heat transfer areas and better capillary forces compared to any other modified surface using traditional micromachining.

TiO_2 materials have received increased attention for their

*Corresponding author (email: xujia@ncepu.edu.cn; xjl@ncepu.edu.cn)

promising applications, including photovoltaics, photocatalysts, photo-/electrochromics and sensors [12]. As continued breakthroughs are made in the preparation of TiO_2 nanotube arrays (NTAs), several studies have indicated that TiO_2 nanotubes can significantly enhance the performance of TiO_2-based devices [13]. Recently it was demonstrated that a TiO_2 NTA interface can intensify heat transfer in the pool boiling process compared with pure Ti metal [14]. However, the critical heat flux (CHF), which limits the maximum power density that can be handled by a boiling heat transfer device, was not reported. The CHF has a significant impact on many energy conversion and utilization processes, so obtaining the CHF of nanomaterial-coated surfaces in pool boiling is important. As a result of the nanoscale size of the material, its morphology can change significantly from environmental impacts like oxidation and stress. The boiling process produces high temperatures on the heating surface and intense nucleation and release of air bubbles. This probably is a challenge for the nanomaterial-coated surfaces. Research on nanomaterial-coated surfaces for the intensification of heat transfer in the pool boiling process is currently in its infancy. To the best of our knowledge, the duration of nanomaterials used for enhanced pool boiling has been far less studied. Here we report the study on the pool boiling of saturated water on surfaces covered with three types of vertically oriented TiO_2 NTAs characterized by their anodization times during fabrication. Significant heat transfer enhancements in both the CHF and the heat transfer coefficient (HTC) were observed compared with boiling on bare Ti metal. Using TiO_2 NTAs, the incipient boiling wall superheat was decreased by about 11 K. It was determined that different heat transfer enhancements between the three types of TiO_2 NTAs can be attributed to the different degrees of deformation in the nanostructure during boiling. The long-term performance of the TiO_2 NTAs was also investigated.

2 Experiment

The apparatus used in this study consisted of a viewing chamber filled with water that was used to observe the pool boiling performance directly, a heating unit and a Ti-Cu composite cylinder featuring TiO_2 NTAs soldered on top of the heating unit. Voltage signals from thermocouples embedded in the heating unit were recorded using a computer-controlled, high-speed data acquisition system (Agilent 34970A). Figure 1(a) presents a schematic of the experimental setup.

The raw materials used for fabricating the heating surfaces with highly-ordered TiO_2 NTAs were Ti-Cu composite bars (Beijing Cuibolin Non-Ferrous Technology Developing Co., Ltd.). The Ti-Cu bars featured a Cu core and a 1 mm thick Ti shell. Ti-Cu composite cylinders with thicknesses of 2.0 mm and basal diameters of 12.0 mm were cut from the surface layer of the Ti-Cu composite bars. The cylinders resembled coins where one face of the coin was Ti and the other was Cu. The thicknesses of Ti and Cu were both 1.0 mm, as shown in Figure 1(b). The face featuring Ti was used to prepare the TiO_2 NTAs. The Cu face was sol-

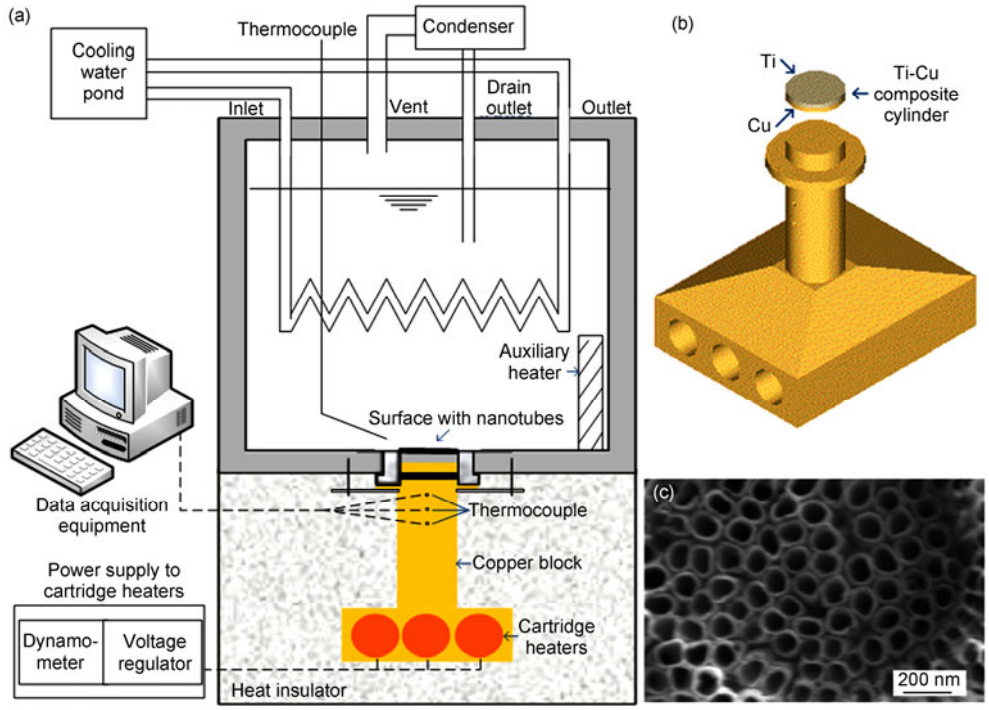

Figure 1 Schematic illustration of (a) the pool boiling experimental setup, (b) Cu block and Ti-Cu composite cylinder, (c) SEM image of the top view of a TiO_2 NTA.

dered to the copper block used as the heating unit in the experiments.

After cleaning with ethanol, the Ti-Cu composite cylinders were subjected to anodization using a 0.50 wt% NH_4F ethylene glycol solution with 2 vol% H_2O. Only the Ti face of the Ti-Cu composite cylinders was exposed to the electrolytes, while the Cu face was sealed to prevent erosion. Three types of samples anodized at 40 V for 1.5, 2 and 3 hours resulted in the formation of three different types of TiO_2 NTAs, denoted as type I, type II and type III, respectively. To obtain crystalline TiO_2 nanotubes with better stability and thermal conductivity, all the samples were then annealed in oxygen above 525°C. Scanning electron microscopy (SEM) characterizations for the top views of the fabricated TiO_2 NTAs showed similar morphologies for all the three types, with inner and outer diameters of 80 nm and 100 nm, respectively, as shown in Figure 1(c). Due to the substrate for TiO_2 nanotubes was bulk material, general techniques for preparing samples in SEM characterization would cause huge impact on the surface morphology. And only average heights were meaningful in our experiments because the research here on the heat transfer enhancement was an overall average effect of macro-scaled collections of a huge number of TiO_2 nanotubes. Thus, there indeed were lots of difficulties for in-situ characterizing the average heights of the TiO_2 NTAs. According to the results of TiO_2 NTAs fabricated on the Ti foils, there was a monotonic relationship between the heights of the TiO_2 NTAs and the anodization time used in the fabrication [15]. Hence, anodizationtime was therefore used to distinguish the prepared samples in this paper.

Figure 1(b) presents a schematic of the heating block instrumentation. The heating block was made of copper. In the bottom of the heating block there were three holes (diameter of 8.0 mm) where three cartridge heaters were inserted that provided the heating power to the copper block. A maximum power of 120 W at an applied AC voltage of 220 V could be provided by each heater. The power supply system consisted of a 220 V voltage stabilizer, a voltage transformer and a power meter, as shown in the right portion of Figure 1(a). Three equally spaced K-type thermocouples were embedded in the copper block, with their values denoted as T_1, T_2 and T_3. They were used to measure the axial heat flux and deduce the temperature of the boiling surface, T_{wall}. At the top of the copper block was a round plate (diameter of 12.0 mm) that was connected to the Cu face of the Ti-Cu composite cylinders with a solder. A protruding edge under the round plate was used to support Telfon between the plate and the viewing chamber.

The structure of the pool boiling chamber is shown schematically in Figure 1(a). The transparent glass chamber (200×200×270 mm) contained the experimental equipment and water. In the experiments, the chamber was filled with deionized water until the level was higher than the boiling surface by 200 mm. The setup was similar to another viewing chamber used in ref. [16], with a small difference that a round, not a square hole, was drilled in the center of the stainless steel plate to expose the testing surfaces on top of the copper block. Teflon and epoxy glue were used to fill spaces between the steel and copper blocks for sealing. Each side of the heating block under the plate was insulated with high-temperature insulation fiberglass to ensure one-dimensional heat flow to the boiling surface. An auxiliary heater was located in a corner of the glass chamber, which was used to heat the water to the saturation temperature at the beginning of the experiments. A reflux condenser was used to cool the vapour induced by boiling and was open to atmosphere to maintain atmospheric pressure in the glass chamber. The temperature of the pool liquid, T_{water}, was monitored using a K-type thermocouple immersed in the water, about 5 mm above the boiling surface.

Prior to the boiling experiments, a degassing procedure was adopted. The auxiliary heater was used to vigorously boil the water for one hour to remove non-condensable gases. During the boiling experiment, the power conveyed to the heating unit gradually increased. A steady state was considered if variation in the copper block temperature was less than 1°C over ten minutes. T_1, T_2 and T_3 were then recorded under the given power. Finally, two parameters were obtained: the surface superheat ΔT_{sat} defined as $\Delta T_{sat}= T_{wall}-T_{sat}$ (T_{wall}=boiling surface temperature, T_{sat}= saturation temperature of water, 100°C), and the heat flux q. With these two parameters the HTC, h, defined as $h=q/(T_{wall}-T_{water})$, could be calculated. For the well thermal insulation of the copper block in our experiments, the assumption of one-dimensional thermal conduction within the cylindrical portion of the copper block (between the lowest thermocouple position and the boiling surface) was adopted. Based on the one-dimensional heat conduction equation, the heat flux was calculated using the gradient of the temperature profiles in the copper block, $q=-k_s \left.\frac{\mathrm{d}T}{\mathrm{d}z}\right|_{\text{testing surface}}$, where k_s is the thermal conductivity of copper, $\left.\frac{\mathrm{d}T}{\mathrm{d}z}\right|_{\text{testing surface}}$ is the temperature gradient at the testing surface and z is the coordinate perpendicular to the testing surface. A least squares correlation of temperature versus z was described as $T=\alpha_0+\alpha_1 z$, where α_0 and α_1 are constants derived based on T_1, T_2 and T_3 (see Figure 1(a)). This method of data processing was also used in previous reports [16]. A modification was made to deduce the temperature of the boiling surface, T_{wall}. Resulted from the structure of the heating unit and experimental samples, k_s should be the thermal conductivity of titanium when z= 1.0 mm under the testing surface. The heat flux uncertainty was estimated to be less than 6.0%. The Twall had maximum uncertainty of

0.3°C. After performing the standard uncertainty analysis, we obtained the maximum relative uncertainty of h of 8.52%.

3 Results and discussion

Typical boiling curves of a plain Ti surface and the TiO_2 NTAs are shown in Figure 2(a). Boiling on a plain Ti surface served as a comparison to evaluate the improvement of boiling performance induced by the TiO_2 NTAs. It is evident that TiO_2 NTAs significantly enhanced heat transfer. The incipient boiling wall superheat of the TiO_2 NTA covered surfaces, marked as A in the boiling curves, and were lower than that of the plain surface by about 11 K. At low heat flux conditions (below approximately q=10 W/cm^2, B point in the boiling curves), there were small differences in the boiling curves among the three types of TiO_2 NTAs. Their boiling curves were different as the heat flux increased. Under these conditions, the type III TiO_2 NTA had the best thermal performance in the types. However, as the boiling progressed, the performance of the type III TiO_2 NTA decreased, but was still superior to that of the plain Ti surface.

CHF refers to a sudden, dramatic increase in the wall superheat at a certain heat flux induced by the existence of a continuous vapour film between the liquid and the heated surface. The CHF in our experiment was 128.8 W/cm^2 for boiling heat transfer on the plain surface. This value was higher than the CHF provided by the well-known Zuber correlation [17] of ~110 W/cm^2 for the saturation pool boiling heat transfer on a large, plain surface with water as the working fluid. Despite this, our result was reasonable for the following reasons. First, CHF is not considered to remain constant, and increases as heater size decreases [18]. Second, Rainey and You recommended using the experimentally determined curve of $q_{CHF,small}/q_{CHF,large}$, which was 1.22 for saturated water boiling, where $q_{CHF,small}$ and $q_{CHF,large}$ are the CHFs for small and large heater sizes, respectively [19]. Therefore, the predicted CHF for saturation pool boiling, considering the small heater size effect, would be 135 W/cm^2. Using the two theories mentioned above, the CHF obtained in this study for saturation pool boiling on a plain surface is within the expected range. In our experiments, the CHF values for the TiO_2 NTAs were between 179.3–186.7 W/cm^2, and exhibited no apparent relationship with the type of NTA. The highest CHF was 186.7 W/cm^2 and comparable to the CHF reported in the literature for pooling boiling on Si and Cu nanowire arrays (~200 W/cm^2) [10].

Dependency of the measured HTCs on heat fluxes for the plain surface and the TiO_2 NTAs is presented in Figure 2(b). It is evident that the HTCs for all three kinds of TiO_2 NTAs are higher than the HTC for the plain surface. This result corresponds to the heat transfer enhancement effect observed in the boiling curves. For the plain surface, as the heat flux increased from zero to the CHF, the heat transfer coefficient increased. The same overall upward trends also existed in the HTC curves for surfaces covered by types I and II TiO_2 NTAs. But, for type III TiO_2 NTA-coated surface, during the late stages of the boiling experiment, the HTC decreased gradually to lower than the HTC for type II TiO_2 NTA-coated surface. The largest HTC was 6.22 W/cm^{2}K from type II TiO_2 NTA. This HTC was nearly twice the HTC of the plain surface.

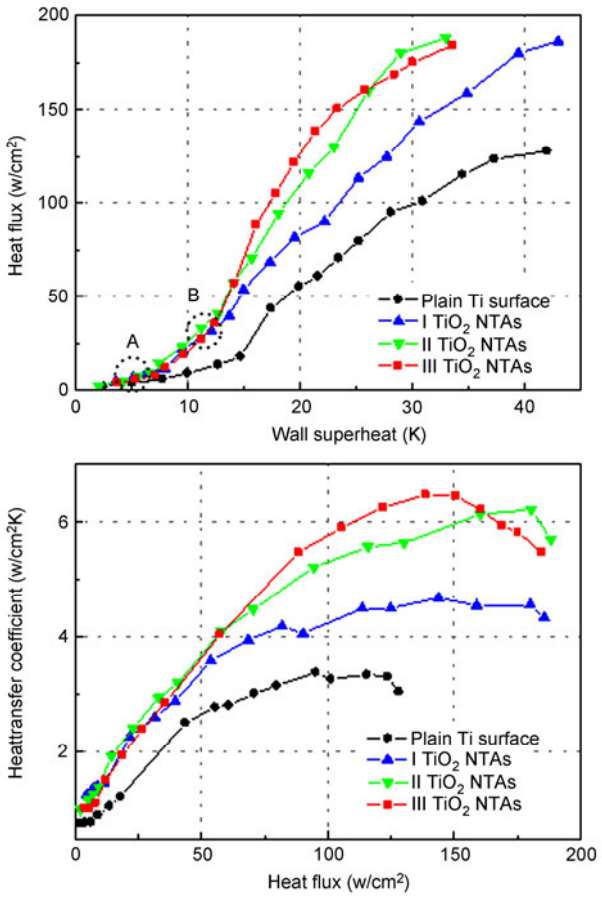

Figure 2 (a) Boiling curves and (b) dependence of measured heat transfer coefficient on heat flux for the plain Ti and the three types of TiO_2 NTAs.

The enhancement of pool boiling heat transfer on nano-textured surfaces is generally attributed to the combined effects of the superhydrophilicity of some kinds of nano-materials, increased surface area, increased nucleation site density and capillary-assisted liquid flow towards the nanowires or nanotubes. Superhydrophilic wetting behaviour of TiO_2 NTAs has been widely reported [20]. CHF is generally believed to increase as contact angle decreases [21]. Based on this, wetting behaviour of the TiO_2 NTA-coated surfaces better than the plain surface likely contributed to the enhancement of pool boiling heat transfer. Enhancement of boiling heat transfer on nano-textured surfaces essentially depends on the balance between the liquid suction capability towards the porous structure and the vapour release re-

sistance to the pool liquid environment. The liquid supply and vapour release occur as a liquid-vapour counterflow, resisting the motions of each other. To the best of our knowledge, there is no quantitative formula to characterize the vapour flow on a nano-textured surface. A porous covering model was used here. Meléndez and Reyes proposed a correlation to compute the vapour flow rate escaping from porous coverings [22]:

$$m = \frac{\pi}{128}\left(\frac{\rho_g \sigma}{\mu_g}\right)\left(\frac{\varepsilon d_p^3}{\delta}\right), \quad (1)$$

where ρ_g and μ_g are the vapour density and viscosity, respectively, σ is the surface tension force and ε, δ and d_p are the porosity, thickness and pore diameter of the porous covering, respectively. A large vapour mass flow rate, m, produces a lower resistance for vapour release and aids heat transfer. Here, δ, d_p and ε are the thickness of the TiO_2 NTA, the dimension of the sub-micrometre cavities in the NTA and the porosity of microscale cavities, respectively. According to the fabrication process and SEM characterizations of the TiO_2 NTAs before the boiling experiment, the three types of TiO_2 NTAs have approximately the same values of d_p and ε and different values of δ. At the beginning of the experiment, i.e. before point A in boiling curves (see Figure 2), natural convection was the mechanism for heat transfer and no bubbles were formed. The effect of nanostructures for enhancing heat transfer was not obvious during this stage. Therefore, there was little difference observed among the nano-textured surfaces and plain smooth surface. As the heat flux increased, due to the better wetting and porous structure of the TiO_2 NTAs, wall superheats firstly met the TiO_2 NTA's requirements for the activation of vapour bubbles. So the onset of nucleate boiling for the TiO_2 NTA-coated surfaces was earlier than it for the plain surface. Despite the wide difference in the vapour mass flow rate, m, resulting from the different δ values for the three types of TiO_2 NTAs, the bubbles nucleating at the heated surface and then escaping to the pool liquid were discrete at the initial stage of nucleate boiling. This resulted in the boiling curves between points A and B being similar to each other, making it difficult to distinguish which NTA type was better. Beyond point B, as nucleated boiling developed, bubbles began to merge to form columns. When the heat flux was less than 150 W/cm^2, the heat transfer enhancement effect of type III TiO_2 NTA was the best, while type II was second and type I was the last. This result was seemingly inconsistent with the m determined from eq. (1), since type I NTA had the smallest δ value. But the result was reasonable for the following reasons. For porous surfaces fabricated using traditional micromachining technology, the parameters are fixed during boiling. Even if oxidation or some other form of corrosion occurs, it will not cause large changes in the parameters. Due to the scale of nanomaterials, their morphology can be changed significantly as a result of violent nucleate boiling, making their parameters variable during boiling. Figures 3(a)–(c) present the SEM characterizations of the three types of TiO_2 NTAs after the pool boiling experiments. There were more defects after pool boiling than in the NTAs before boiling. A large amount of debris lay on top of the NTAs, resulting from damage to the nanotubes. This damage means that parts of the TiO_2 nanotubes had collapsed and more sub-micrometre cavities had been activated in the NTAs. In other words, as boiling developed, d_p and ε increase, but δ decreased for all three types of TiO_2 NTAs. This made the value of m larger than it was initially for each kind of the TiO_2 NTAs. This is undoubtedly conducive to boiling heat transfer. It can also be seen that the damage to the NTAs is more serious in the order type I < type II < type III. For type III TiO_2 NTA, nanotube fragments almost completely covered the top of the NTA. By noting that these SEM characterizations were performed after the boiling experiments, it can be deduced that during the boiling process, the increases in d_p and ε for type III were the largest among the three types of TiO_2 NTAs. It is likely that the longer the NTA, the poorer the stability of the morphological structure during the intense heating and nucleating bubbles process. Further, according to eq. (1), an increase in d_p can cause a rapid increase in m. Therefore, in a certain range of heat fluxes, the heat transfer enhancement performance of type III TiO_2 NTA is better than that of type II, and performance of type II is better than that of type I. However, as shown in Figure 3(c), such serious debris cover will inevitably lead to a disappearance of the nanomaterials effect for enhancing heat transfer, corresponding to the degradation in the boiling curve of type III TiO_2 NTA. Although the above analysis is qualitative, it is considered reasonable that the only difference between the three types is their heights which monotonically depends on the anodization time. The exact value for the average height of TiO_2 NTA is necessary in quantitative analysis, which is our goal in the future research.

The long-term performance is also an important parameter to evaluate in the enhancement of the pool boiling performance of a nano-textured surface. It took approximately 6–7 h to complete the boiling experiments. During the remainder of the day, the tested surface was soaked in water. The boiling experiment was repeated on the next day. This cycle was repeated for 10 d. To ensure that the nanotubes were not subjected to the large increase in the wall superheat at the CHF, the maximum heat flux used in these experiments was smaller than the CHF obtained before. The boiling curves obtained on the tenth day for type II and type III TiO_2 NTA-coated surfaces are shown in Figure 4(a). The boiling curves obtained on the first day are also plotted for comparison. The heat transfer performance on the heated surface covered by type II TiO_2 NTA changed little in all the heat flux ranges. A reduction in the pool boiling performance on the heated surface covered by type III TiO_2 NTA after 10 d of operation was apparent. The reason for

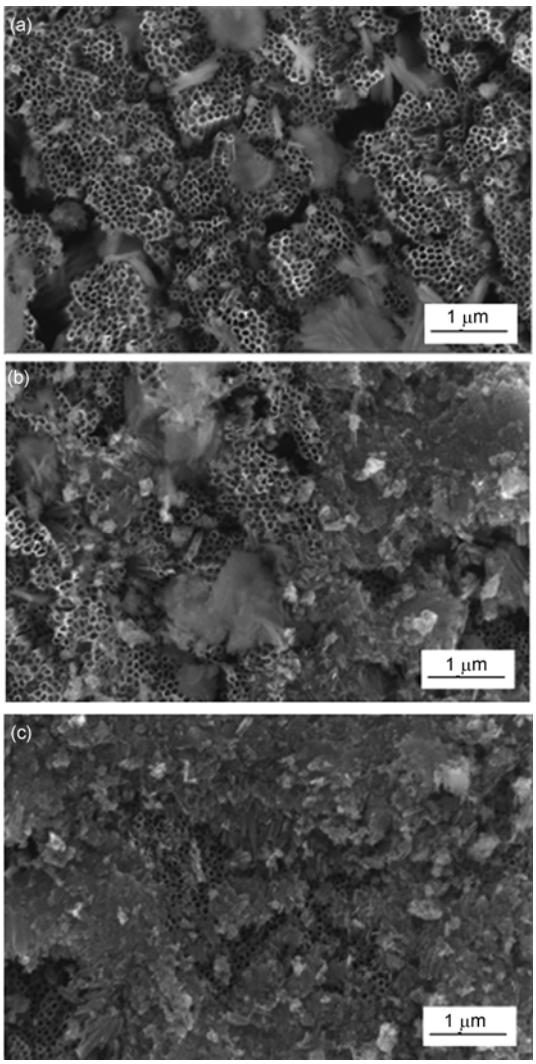

Figure 3 SEM images of types (a) I; (b) II; (c) III TiO_2 NTAs after the boiling experiment.

this was clear from the SEM characterization of type III TiO_2 NTA after 10 d of operation. As shown in Figure 4(b), some pieces of the NTA were peeled off the Ti substrate and a large gap existed between some pieces of the NTA and the Ti substrate. Such serious destruction of the TiO_2 NTA likely caused the reduction in the pool boiling performance.

4 Conclusions

In summary, pool boiling of saturated water on ordered, vertically-oriented TiO_2 NTAs has been performed. The TiO_2 NTAs were fabricated using potentiostatic anodization of Ti in fluoride ion containing baths in combination with non-aqueous, organic, polar electrolytes. Three types of TiO_2 NTAs were obtained as the result of different anodization times. Significant enhancement of pool boiling heat transfer on the TiO_2 NTAs was observed compared with a

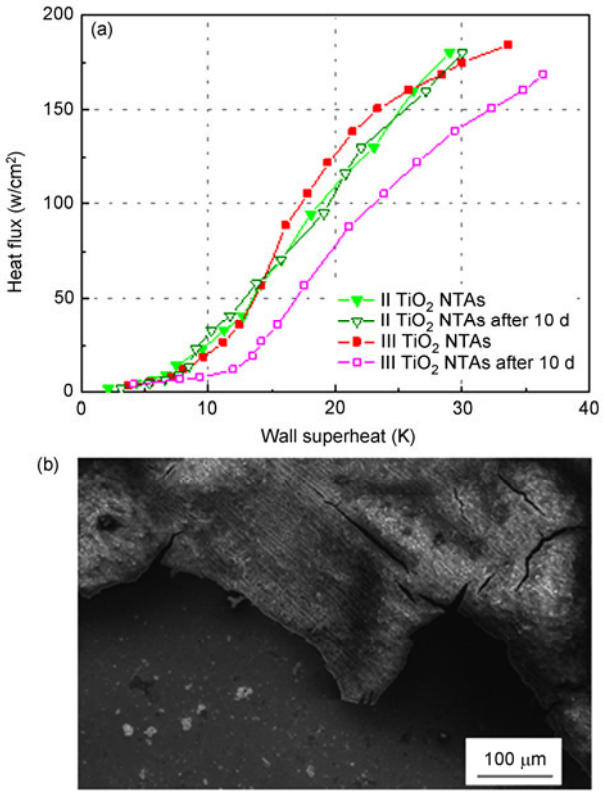

Figure 4 Long-term performance of the TiO_2 NTAs. (a) Boiling curves for types II and III TiO_2 NTAs before and after 10 d of operation; (b) SEM image of type III TiO_2 NTA after 10 d of operation.

plain Ti surface. For example, the incipient boiling wall superheat was decreased by a maximum of 11 K, the HTC at the CHF condition could also be 1.86 times that of the plain surface and an increase in the CHF of nearly 58 W/cm^2 was obtained. Besides the unique properties of NTAs, such as high nucleation site density, superhydrophilicity and enhanced capillary pumping effect, the effect of having unfixed morphological parameters during boiling can also be an advantage for enhanced heat transfer. But serious deformation, which occurred in the TiO_2 NTA with an anodization time of 3 h, can also introduce degradation problems. The results suggest that the mechanism for the nanomaterials used for enhancing heat transfer is very complicated, and more intensive researches are need in further work.

This work was supported by the National Natural Science Foundation of China (Grant Nos. 11004054, 50825603, U1034004) and the Fundamental Research Funds for the Central Universities.

1 Thome J R. Enhanced Boiling Heat Transfer. New York: Hemisphere, 1990
2 Mudawar I. Assessment of high-heat-flux thermal management schemes. IEEE T Compon Packag Technol, 2001, 24(2): 122–141
3 Thome J R. Boiling in microchannels: A review of experiment and theory. Int J Heat Fluid Flow, 2004, 25(2): 128–139

4 Kim J. Review of nucleate pool boiling bubble heat transfer mechanisms. Int J Multiphase Flow, 2009, 35(12): 1067–1076
5 Hubner P, Kunstler W. Pool boiling heat transfer at finned tubes: Influence of surface roughness and shape of the fins. Int J Refrig, 1997, 20(8): 575–582
6 Jung J Y, Kwak H Y. Effect of surface condition on boiling heat transfer from silicon chip with submicron-scale roughness. Int J Heat Mass Transfer, 2006, 49(23-24): 4543–4551
7 Li S H, Furberg R, Toprak M S, et al. Nature-inspired boiling enhancement by novel nanostructured macroporous surfaces. Adv Funct Mater, 2008, 18(15): 2215–2220
8 Xu J L, Ji X B, Zhang W, et al. Pool boiling heat transfer of ultra-light copper foam with open cells. Int J Multiphase Flow, 2008, 34(11): 1008–1022
9 Ahn H S, Sinha N, Zhang M, et al. Pool boiling experiments on multiwalled carbon nanotube (MWCNT) forests. J Heat Transfer, 2006, 128(12): 1335–1342
10 Chen R, Lu M C, Srinivasan V, et al. Nanowires for enhanced boiling heat transfer. Nano Lett, 2009, 9(2): 548–553
11 Li C, Wang Z, Wang P I, et al. Nanostructured copper interfaces for enhanced boiling. Small, 2008, 4(8): 1084–1088
12 Diebold U. Structure and properties of TiO_2 surfaces: A brief review. Appl Phys A, 2003, 76(5): 681–687
13 Mor G K, Varghese O K, Paulose M, et al. A review on highly ordered, vertically oriented TiO_2 nanotube arrays: Fabrication, material properties, and solar energy applications. Sol Energy Mater Sol Cells, 2006, 90(14): 2011–2075
14 Chen Y, Mo D C, Zhao H B, et al. Pool boiling on the superhydrophilic surface with TiO_2 nanotube arrays Sci China Ser E-Tech Sci, 2009, 52(6) 1596–1600
15 Shankar K, Mor G K, Prakasam H E, et al. Highly-ordered TiO_2 nanotube arrays up to 220 μm in length: use in water photoelectrolysis and dye-sensitized solar cells. Nanotechnology, 2007, 18(6): 065707
16 Yang Y P, Ji X B, Xu J L. Pool boiling heat transfer on copper foam covers with water as working fluid. Int J Therm Sci, 2010, 49(7): 1227–1237
17 Zuber N. Hydrodynamic Aspects of Boiling Heat Transfer AEC Report. AECU-4439, 1959
18 Lu M C, Chen R K, Srinivasan V, et al. Critical heat flux of pool boiling on Si nanowire array-coated surfaces. Int J Heat Mass Transfer, 2011, 54(25-26): 5359–5367
19 Rainey K N, You S M. Effects of heater size and orientation on pool boiling heat transfer from microporous coated surfaces. Int J Heat Mass Transfer, 2001, 44(14): 2589–2599
20 Miyauchi M, Tokudome H. Super-hydrophilic and transparent thin films of TiO_2 nanotube arrays by a hydrothermal reaction. J Mater Chem, 2007, 17(20): 2095–2100
21 Dhir V K, Liaw S P. Framework for a unified model for nucleate and transition pool boiling. J Heat Transfer, 1989, 111(3): 739–746
22 Meléndez E, Reyes R. The pool boiling heat transfer enhancement from experiments with binary mixtures and porous heating covers. Exp Therm Fluid Sci, 2006, 30(3): 185–192